

6-2011

Change in carbon nanofiber resistance from ambient to vacuum

Shusaku Maeda

Patrick Wilhite

Santa Clara University, pwilhite@scu.edu

Nobuhiko Kanzaki

Toshishige Yamada

Santa Clara University, tyamada@scu.edu

Cary Y. Yang

Santa Clara University, cyang@scu.edu

Follow this and additional works at: <https://scholarcommons.scu.edu/elec>

Recommended Citation

S. Maeda, P. Wilhite, N. Kanzaki, T. Yamada, and C.Y. Yang, "Change in carbon nanofiber resistance from ambient to vacuum," *AIP Advances* 1, 022102 (1-6) (2011). <https://doi.org/10.1063/1.3582812>

Copyright © 2011 American Institute of Physics Publishing. Reprinted with permission.

This Article is brought to you for free and open access by the School of Engineering at Scholar Commons. It has been accepted for inclusion in Electrical Engineering by an authorized administrator of Scholar Commons. For more information, please contact rsroggin@scu.edu.

Change in carbon nanofiber resistance from ambient to vacuum

Shusaku Maeda, Patrick Wilhite, Nobuhiko Kanzaki, Toshishige Yamada,
and Cary Y. Yang

Center for Nanostructures, Santa Clara University, Santa Clara, California 95053, USA

(Received 5 March 2011; accepted 17 March 2011; published online 14 April 2011)

The electrical properties of carbon nanofibers (CNFs) can be affected by adsorbed gas species. In this study, we compare the resistance values of CNF devices in a horizontal configuration in air and under vacuum. CNFs in air are observed to possess lower current capacities compared to those in vacuum. Further, Joule heating due to current stressing can result in desorption of gas molecules responsible for carrier trapping, leading to lower resistances and higher breakdown currents in vacuum, where most adsorbed gaseous species are evacuated before any significant re-adsorption can occur. A model is proposed to describe these observations, and is used to estimate the number of adsorbed molecules on a CNF device. *Copyright 2011 Author(s). This article is distributed under a Creative Commons Attribution 3.0 Unported License.* [doi:10.1063/1.3582812]

I. INTRODUCTION

Nanoscale carbon structures such as carbon nanotube (CNT)¹⁻³ and carbon nanofiber (CNF)⁴⁻⁶ are promising as next-generation on-chip interconnect materials due to their tolerance to electromigration and higher current capacity than copper.^{7,8} CNF can be directionally grown at lower temperature than CNT and has excellent thermal and electrical properties.⁹ Thus, an in-depth understanding of its electrothermal characteristics is necessary for further consideration of its potential for interconnect and other device applications. Previously we studied the temperature dependence of CNF resistance⁶⁻¹⁰ in an attempt to elucidate its electrical transport mechanisms. In this paper, we report the resistance behavior of CNFs under vacuum environment, and compare with its counterpart under ambient conditions. Our results show that adsorption/desorption of gaseous molecules in atmosphere is the dominant mechanism underlying the observed CNF resistance change.

II. DEVICE FABRICATION AND TEST

CNFs were grown using plasma-enhanced chemical vapor deposition (PECVD), with acetylene (C_2H_2) as the carbon source, ammonia (NH_3) as a reducing agent, and nickel (Ni) as catalyst.¹¹ After growth, the CNFs were suspended in isopropyl alcohol, and drop-casted onto a test device consisting of pre-patterned gold (Au) electrodes on a silicon dioxide (SiO_2) substrate. Tungsten (W) was then deposited onto the CNF-Au contact using electron-beam-induced deposition (EBID) for contact improvement,^{12,13} resulting in reduced overall resistance of the device. While contact resistance can be reduced by several orders of magnitude with an applied current, which anneal the contacts through Joule heating,^{7,14} W depositions on the electrodes result in further reduction of contact resistances.⁸ Also, CNFs with W-deposited contacts do not experience resistance change after being subject to successive current stressing, unlike those without W contacts, leading to the conclusion that Joule heating has little effect on W-deposited contacts.⁸

Each device was then subjected to current stressing consisting of a series of progressively increasing constant currents.⁷ In between current stress cycles, when the device is cooled down, low-voltage sweeps were performed to determine the resistance at ambient temperature. During



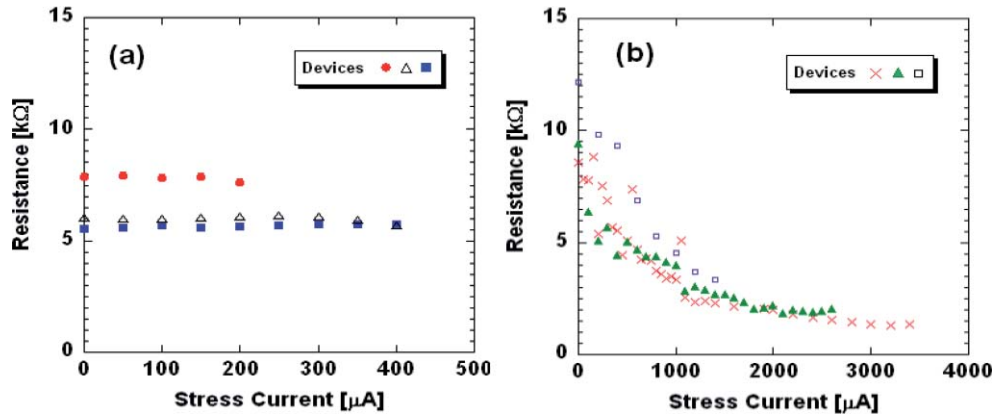


FIG. 1. Resistance of CNF test devices in atmosphere (a), and in vacuum (b). Resistances are recorded after each current stress cycle when the device returns to room temperature. For each device, the final data point corresponds to the last measured stress current/resistance before breakdown.

each stress current cycle, when the device is undergoing Joule heating, the voltage is recorded to yield the resistance at an elevated temperature.^{9,10}

Samples measured under atmospheric conditions were tested using a wafer probe station which utilizes micromanipulators coupled to Kelvin probes. These probes rest on the Au pads of the device while current-voltage (I - V) measurements are performed with a semiconductor parameter analyzer. For vacuum conditions, we used a similar configuration consisting of nanomanipulators with W probe-tips inside the chamber of a scanning electron microscope (SEM), with base pressure of about 1×10^{-4} Pa.

III. RESULTS AND DISCUSSION

In ambient, the average resistance during each stress cycle decreases with increasing stress current, similar to previous observations.^{6,8,10} On the other hand, resistance measured after each stress cycle (at room temperature) shows an almost constant value as shown in Figure 1(a). This behavior is also similar to our previous observations, indicative of carrier trapping and detrapping.⁸ In vacuum, however, the results after each stress cycles show a significant decrease in device resistance, as shown in Figure 1(b).

As we previously reported,¹⁰ the results in ambient suggests that carriers are trapped by defects along the conductive graphitic layers of the CNF at room temperature. In addition to defects, some gaseous species adsorbed on the CNF can also serve as carrier traps, similar to other carbon nanostructures.¹⁵⁻²⁰ The trapped carriers are detrapped as a result of thermal activation by Joule heating when its temperature is increased due to current stressing. In atmosphere, these detrapped carriers are trapped again after the device returns to room temperature. Even though the resistance during each stress cycle decreases from one cycle to the next due to carrier detrapping, it returns to its initial value after cooling down to room temperature and re-trapping carriers. Thus the measured resistance after each stress cycle remains constant until device breakdown, as shown in Figure 1(a). Because the resistance returns to its original value after cooling down to room temperature, the decrease in high-temperature resistance during each stress cycle cannot be due to contact annealing which is irreversible, consistent with our previous observations.⁸

On the other hand, under vacuum conditions, the resistance after each stress cycle decreases with increasing stress current, as shown in Figure 1(b). Thus, resistance measured after each stress cycle in vacuum does not return to their initial value. As in the ambient case, we attribute this behavior to thermal desorption of gaseous molecules absorbed on the CNF in atmosphere, which act as carrier traps in addition to those due to defects proposed previously.¹⁰ However, when desorbed in vacuum through Joule heating, most if not all of these gaseous species are evacuated, preventing re-adsorption onto the CNF and resulting in a continuous decrease in resistance as stress current increases. Further,

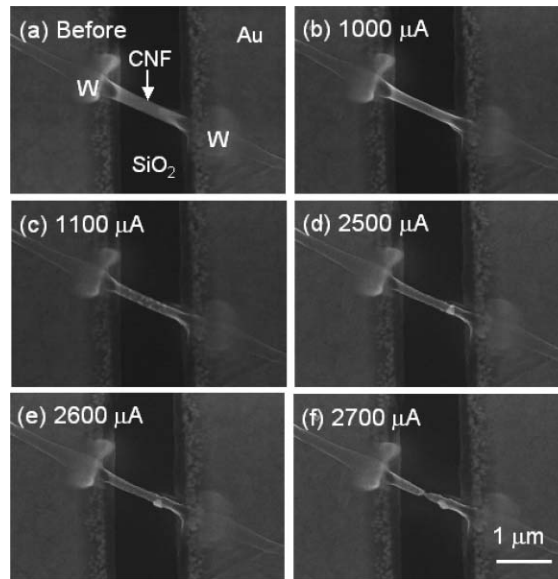


FIG. 2. SEM images of CNF test device before current stressing and after several stress cycles in vacuum: (a) before stress, (b) after 1000 μA , (c) after 1100 μA , (d) after 2500 μA , (e) after 2600 μA , and (f) after 2700 μA (breakdown).

breakdown currents of CNFs in vacuum are much higher than those in ambient (see Figure 1). This is attributed to the much lower concentrations of oxidizing species such as oxygen and water molecules in vacuum, which have been shown to lead to carbon nanotube failure.¹⁵

Figure 2 shows the SEM images of a CNF test device in vacuum. Progressively increasing stress currents were applied to the device, and image scans were performed before and after each stress cycle. Significant structural changes are evident in the outer layers of the CNF after stressing at 1100 μA and higher, and these changes become more pronounced as the device approaches breakdown at 2700 μA . Although the images show damages to the CNF, the resistance of the device continues to decrease until breakdown. Higher-resolution microscopy is needed to investigate these structural changes and is beyond the scope of this paper.

To investigate further the difference in CNF device resistance change after each stress cycle between ambient and vacuum, we performed a series of current stressing experiments on the same device under vacuum and exposed to air after a few stress cycles, as shown in Figure 3. Each data point was obtained after a three-minute stress cycle when the device is cooled down to room temperature. The stress current was increased in 100 μA steps up to 1000 μA for two stages. This upper limit was chosen to avoid damage to the CNF (see Figure 2), in an attempt to isolate the suggested trapping/detrapping phenomenon. For the first two stages, after stressing at 1000 μA , air was introduced into the chamber for 5 and 10 minutes, respectively. Before the third stage, air was reintroduced and the sample was subjected to another series of stress cycles until breakdown at 2700 μA .

The resistance values in Figure 3 show a decrease after successive stress current cycles, and an increase after exposure to air for each of the first two stages. Further, this resistance increase is higher when the air exposure time is longer. Thus, based on the assumption of carrier trapping by adsorbates, the longer exposure time results in more molecules absorbed and consequently more carriers trapped, resulting in higher resistance. This result suggests that trapping by absorbed molecules is likely to dominate that due to defects in CNFs,¹⁰ as the latter is expected to be a much faster process. This finding is also consistent with the continuous resistance decrease with increasing stress current in the third stage (see Figure 3), resulting in more molecules desorbed accompanied by release of carriers. It is less likely that such resistance decrease would occur at such high stress currents (hence high temperatures) if detrapping from defects were the dominant mechanism, since the carriers would have all been detrapped long before reaching these temperatures.

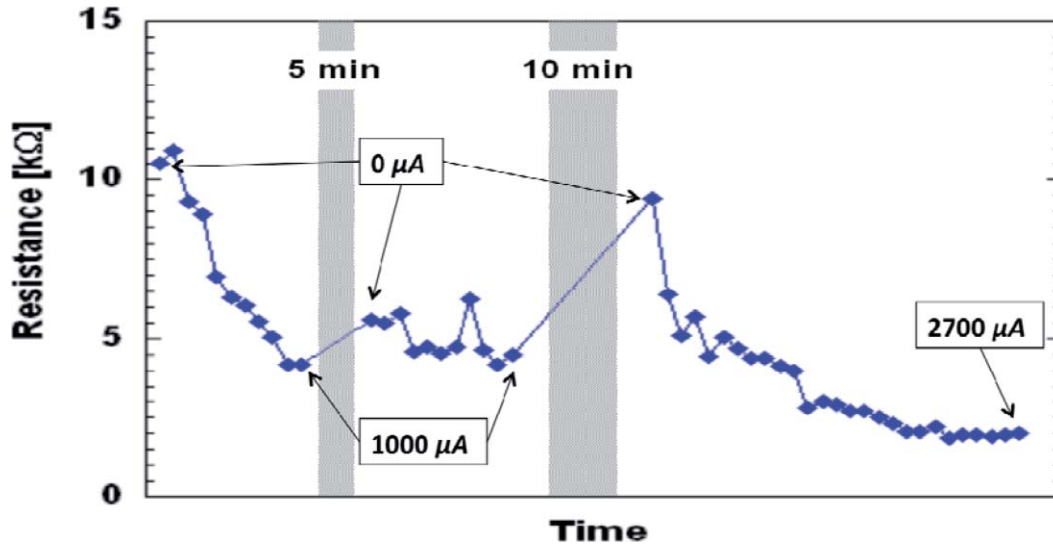


FIG. 3. Resistance of a CNF device in vacuum and under air exposure as indicated by the shaded regions. Resistance values are recorded before current stressing begins and after each stress cycle, up to 1000 μA in 100 μA steps for the first two stages. In the third stage, stressing continues till device breakdown.

IV. ADSORPTION/DESORPTION MODEL

Figure 4 shows a schematic of a model to describe the adsorption/desorption on CNF and the associated carrier trapping/detrapping under ambient and vacuum conditions, as described in Section III. The model assumes the adsorption of one or more gaseous species in atmosphere at room temperature, which desorb via Joule heating of the CNF device under ambient conditions (Figure 4(a)), accompanied by release of carriers into the CNF. Upon cooling down to room temperature, the molecules are re-adsorbed and the resistance returns to its preheated value. If the heating occurs in vacuum (Figure 4(b)), the desorbed molecules are evacuated and the resistance after cooling down remains at the lower value. This adsorption/desorption model is supported by our results shown in Figures 1 and 3, as discussed in Section III.

Our proposed model is consistent with reports on effects of adsorbed molecular species such as O_2 , H_2O , NH_3 , CO_2 , and NO_2 on electrical transport in CNTs.^{15–20} The general trend reported was increased CNT resistance as a result of exposure to reducing species (NH_3 ,^{18,19} CO_2 ¹⁹), while a decrease was observed for oxidizers (O_2 ,¹⁹ NO_2 ²⁰). These results were typically explained based on the assumption that adsorbates act as electron (or hole) donors or acceptors.

Using the model illustrated in Figure 4, and assuming that trapped carriers by adsorbed molecules to be the principal underlying mechanism for our observed resistance behavior, we estimate the number of carriers detrapped during each stress cycle per cm^3 , Δn , as follows.

$$\Delta\sigma = q(\Delta n)\mu \quad (1)$$

$\Delta\sigma$ is the change in conductivity due to carrier detrapping, extracted from the difference in device resistance in ambient between heated (during current stressing) and cooled (after current stressing) states, q is the electron charge, and μ is the carrier mobility. The measured resistances at a stressing current of 400 μA is used for this estimation. We assume the mobility value for semiconducting CNTs ($\sim 100,000 \text{ cm}^2/\text{V}\cdot\text{s}$)²¹ and scale it by the ratio of the conductivity of our CNF ($2.6 \times 10^2 \text{ S/cm}$), obtained using four-point probe measurement, to that of the reported CNTs ($3.8 \times 10^5 \text{ S/cm}$),²¹ such that $\mu_{\text{CNF}} = \mu_{\text{CNT}} (\sigma_{\text{CNF}}/\sigma_{\text{CNT}}) \sim 68 \text{ cm}^2/\text{V}\cdot\text{s}$. μ_{CNF} is assumed to be constant for this temperature variation. For this CNF device, Δn is then estimated to be $4 \times 10^{18} \text{ cm}^{-3}$, from the difference in resistance between heated and cooled states. From the CNF volume in this device, estimated to be $1.3 \times 10^{-13} \text{ cm}^3$ from SEM images, the number of detrapped carriers ΔN due to Joule heating of this device at this stressing current is then 5×10^5 . If we consider the CNF surface to be

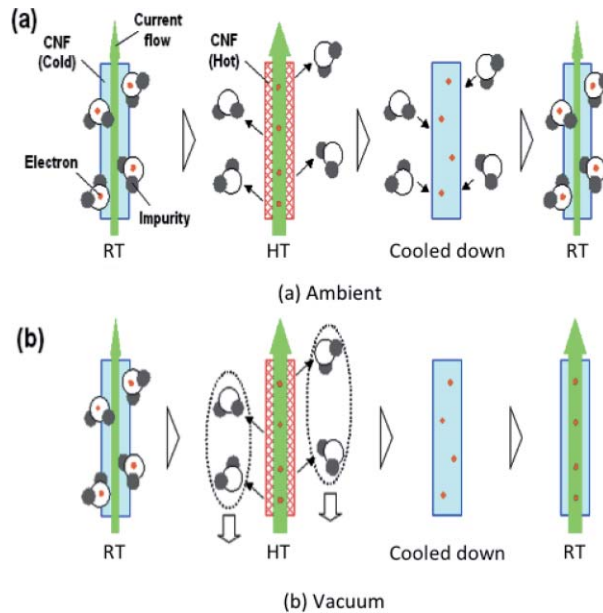


FIG. 4. Model of adsorption/desorption of molecules on CNF and its role in carrier trapping and detrapping in ambient (a) and in vacuum (b). RT and HT stand for room and high temperatures, respectively.

a graphene sheet, with atomic density $3.8 \times 10^{15} \text{ cm}^{-2}$, the number of surface carbon atoms on this CNF is 9.45×10^7 , yielding a surface carbon ratio to ΔN of ~ 190 . If we further assume that one carrier is released by one desorbed molecule, then this ratio infers that there is approximately one adsorbed molecule present on this CNF per 190 surface carbon atoms.

While the result of this estimation does not definitively point to a specific adsorbed species, the fact that exposure to O_2 (electron acceptors) was reported to result in decreased resistance¹⁹ leads us to believe that oxygen in atmosphere is not likely to be the cause of our observed difference in resistance between room and high temperatures. On the other hand, water vapor has been reported to increase resistance in small concentrations for single-walled CNT mats.¹⁷ The same authors also found that degassing while heating their CNT mats resulted in reduced resistance. As CO_2 gas is also present in atmosphere and exposure to it was reported to increase the multi-walled CNT resistance,¹⁹ it is possible that CO_2 and/or water vapor in atmosphere are responsible for the observed resistance behavior of our CNF devices.

V. CONCLUSION

We have shown that CNF electrical properties are degraded by adsorbed gaseous species in atmosphere, with higher resistance and lower current capacity than those in vacuum. These adsorbed molecules can be desorbed through Joule heating, resulting in a decrease in resistance. The resistance returns to its original value due to re-adsorption of these molecules. However, this resistance recovery is not observed in vacuum. A model is proposed to describe such apparent adsorption/desorption phenomenon, and the number of desorbed molecules is estimated from the observed difference in resistance between room and elevated temperatures.

ACKNOWLEDGMENTS

The authors acknowledge the technical support from Hitachi High Technologies America. They are grateful to Philip D. Rack and David C. Joy of the University of Tennessee for their advice on tungsten depositions. This work was supported by the United States Army Space and Missile

Defense Command (SMDC) and carries Distribution Statement A, approved for public release, distribution unlimited.

- ¹ F. Kreupl, A. P. Graham, G. S. Duesberg, W. Steinhogel, M. Liebau, E. Unger, and W. Honlein, *Microelectronic Engineering*, **64**, 399 (2002).
- ² J. Li, Q. Ye, A. M. Cassell, H. T. Ng, R. Stevens, J. Han, and M. Meyyappan, *Appl. Phys. Lett.*, **82**, 2491 (2003).
- ³ M. Nihei, A. Kawabata, D. Kondo, M. Horibe, S. Sato, and Y. Awano, *Jpn. J. Appl. Phys.*, Part 1 **44**, 1626 (2005).
- ⁴ L. Zhang, D. Austin, V. I. Merkulov, A. V. Meleshko, K. L. Klein, M. A. Guillorn, D. H. Lowndes and M. L. Simpson, *Appl. Phys. Lett.*, **84**, 3972 (2004).
- ⁵ A. V. Melechko, V. I. Merkulov, T. E. McKnight, M. A. Guillorn, K. L. Klein, D. H. Lowndes, and M. L. Simpson, *J. Appl. Phys.*, **97**, 041301 (2005).
- ⁶ Q. Ngo, T. Yamada, M. Suzuki, Y. Ominami, A. M. Cassell, J. Li, M. Meyyappan, and C. Y. Yang, *IEEE Trans. Nanotech.*, **6**, 688 (2007).
- ⁷ H. Kitsuki, T. Yamada, D. Fabris, J. R. Jameson, P. Wilhite, M. Suzuki, and C. Y. Yang, *Appl. Phys. Lett.*, **92**, 173110 (2008).
- ⁸ T. Saito, T. Yamada, D. Fabris, H. Kitsuki, P. Wilhite, M. Suzuki, and C. Y. Yang, *Appl. Phys. Lett.*, **93**, 102108 (2008).
- ⁹ T. Yamada, T. Saito, D. Fabris, and C. Y. Yang, *IEEE Elec. Dev. Lett.*, **30**, 469 (2009).
- ¹⁰ T. Yamada, H. Yabutani, T. Saito, and C. Y. Yang, *Nanotechnology*, **21**, 26707 (2010).
- ¹¹ B. A. Cruden, A. M. Cassell, Q. Ye, and M. Meyyappan, *J. Appl. Phys.*, **94**, 4070 (2003).
- ¹² P. D. Rack, J. D. Fowlkes, and S. J. Randolph, *Nanotechnology*, **18**, 465601 (2007).
- ¹³ S. J. Randolph, J. D. Fowlkes, and P. D. Rack, *Crit. Rev. Solid State Mater. Sci.*, **31**, 55 (2006).
- ¹⁴ T. Yamada, T. Saito, M. Suzuki, P. Wilhite, X. Sun, N. Akhavantafsi, D. Fabris, and C. Y. Yang, *J. Appl. Phys.*, **107**, 044304 (2010).
- ¹⁵ P. G. Collins, M. Hersam, M. Arnold, R. Martel, and Ph. Avouris, *Phys. Rev. Lett.*, **86**, 3128 (2001).
- ¹⁶ G. U. Sumanasekera, C. K.W Adu, S. Fang and P. C. Eklund, *Phys. Rev. Lett.*, **85** 1096 (2000).
- ¹⁷ A. Zahab, L. Spina, and P. Poncharal, *Phys. Rev. B*, **62**, 10000 (2001)
- ¹⁸ S. G. Wang, Q. Zhang, D. J. Yanga, P. J. Sellin and G. F. Zhong, *Diamond and Related Materials*, **13**, 1327 (2004).
- ¹⁹ K. G. Ong, K. Zeng, and C. A. Grime, *IEEE Sensors J.*, **2**, 2 (2002).
- ²⁰ C. Cantalini, L. Valentini, L. Lozzi, I. Armentano, J. M. Kenny and S. Santucci, *Sensors and Actuators B*, **93**, 333 (2003).
- ²¹ T. Dürkop, S. A. Getty, E. Cobas, and M. S. Fuhrer, *Nano Lett.*, **4**, 35 (2004).